A Prediction of Pedestal Formation in *H*-mode Tokamak Plasma by Using The Full Calculation of The Radial Electric Field in BALDUR Code

Pianroj Y[1]*, Chatthong B[2], Onjun T[2], Werapun W[1], Promping J[3], and Picha R[3]

[1] Faculty of Sciences and Industrial Technology, Prince of Songkla University Surat Thani Campus, Surat-Thani, 84000, Thailand

[2] School of Manufacturing System and Mechanical Engineering, Sirindhorn International Institute of Technology, Thammasat University, Pathum Thani, 12121, Thailand

[3]Thailand Institute of Nuclear Technology (Public Organization), Nakhon-Nayok, 26120 Thailand

*Corresponding Author: yutthapong.p@psu.ac.th, Tel. +6677 355040, Fax. +6677 355041

Abstract

In this work, a prediction of pedestal formation in *H*-mode tokamak plasma by using the full calculation of the radial electric field (E_r) is performed with three terms of E_r (the pressure gradient, the poloidal velocity, and the toroidal velocity). It is used to compute the important candidate for the edge turbulence stabilization, named the $\omega_{E\times B}$ flow shear. This full calculation is combined to the model for predicting pedestal formation in *H*-mode tokamak plasma based on suppression of anomalous transport that using the $\omega_{E\times B}$ flow shear and the magnetic shear. All calculations are developed and tested in BALDUR integrated predictive modeling code. The simulations with time evolution of plasma current, ion and electron temperature, and particle and impurity density profiles are compared to the experimental profiles of 10 DIII-D *H*-mode discharges. To validate the agreement between the simulation results and the corresponding experiment results, the statistical analysis, including root mean square (RMS%) and offset%, are carried out. The results show that the predicted plasma profiles yield overprediction.

Keywords*:* a radial electric field, tokamak plasma, pedestal, *H*-mode, and BALDUR code.

1. Introduction

Since the high confinement mode (*H*-mode) of tokamak plasmas has been discovered. It is generally provide high temperature and excellent energy confinement time. Typically, the energy content in *H*-mode regime is approximately twice the energy contained in an *L*-mode regime, for the similar plasma with the same input power [1]. Thus, many of burning plasma experiments, not only the Doublet III-Device (DIII-D), Tokamak Fusion Test Reactor (TFTR), and Joint European Torus (JET) were tested in the *H*-mode regime, but also the biggest tokamak, named the International Thermonuclear Experiment Reactor (ITER) [2] is designed to operate in this regime, too.

It is known that the improved performance of *H*-mode results mainly from the formation of an edge transport barrier (ETB) [3], called the pedestal. It is widely believed that a pedestal is

the reduction of a pedestal transport, which can occur due to a stabilization or decorrelation of microturblence in the edge plasma. The stabilization mechanisms, which can suppress turbulent modes, have to take into account the different dynamical behaviors of the various species in the plasma. The first candidate is the magnetic shear stabilization, which is reduced only in the region where the magnetic shear exceeds its threshold. The second candidate is the $\omega_{E\times B}$ flow shear which is the function of the radial electric field (E_r). It can suppress turbulence by linear stabilization of turbulent modes, and in particular by non-liner decorrellation of turbulence vortices [4-6], thereby reducing transport by acting on both the amplitude of the fluctuations and the phase between them [7].

Theoretically, the calculation of $\omega_{E\times B}$ flow shear requires information of the E_r, which can be calculated from three terms, pressure gradient ($\partial p_i / \partial r$), the poloidal velocity (v_θ), and the toroidal velocity (v_ϕ), as shows in Eq. (9). As a result, it is crucial to develop a model for predicting toroidal velocity in order to predict the ETB formation in *H*-mode, so the previous work, Pianroj Y, et al. [8-9] performed the model for predicting the pedestal, which based on suppression of anomalous transport using magnetic shear and $\omega_{E\times B}$ flow shear. However, the calculation of $\omega_{E\times B}$ flow shear ignored the toroidal velocity. After the toroidal velocity model in Ref. [10] was developed and implemented to the integrated predictive modeling code BALDUR [11].

In this work, the full calculation of the radial electric field, which consists of three terms, is used to calculate the $\omega_{E\times B}$ flow shear then it is substituted to the suppression model, which composed of two candidates (magnetic shear and $\omega_{E\times B}$ flow shear), for predicting the pedestal formation in experimental results of 10 DIII-D *H*-mode discharges. Thus, this work is organized as follows; the next section is a brief description of BALDUR code, the anomalous core transport model (Mixed B/gB), the suppression model, and the toroidal velocity model. The third section is the results and discussion, also conclusion is in the final section.

2. BALDUR code

The BALDUR integrated predictive modeling code [11] is called a 1.5 dimensional code because the transport equations are one-dimensional flux-surface-averaged equations, in which metric elements describe the effects of the two dimensional shapes on the magnetic flux surfaces. Integrated 1.5 dimensional codes are used when the magnetic flux surfaces are closed and when the transport along magnetic field lines is much larger than the transport across the field lines. BALDUR uses theory-based and empirical models to compute self-consistently the source neutral beam injection (NBI) heating, nuclear reaction, radio frequency (RF heating), sink (impurity radiation), energy and particle transport fluxes, magnetohydrodynamic equilibrium, and large scale instabilities (sawtooth oscillations). The BALDUR simulations have been used to predict the time evolution of plasma profiles including electron and ion temperature, hydrogen and impurity densities, safety factor, neutrals and

fast ions, for *L*-mode and *H*-mode discharges of conventional tokamaks. BALDUR simulations have been extensively compared with experimental data on plasma, and have yielded overall agreements with about a 10% relative RMS deviation [12-13]. In the BALDUR code, fusion heating power is determined by the nuclear reaction rate together with a Fokker-Planck package that computes the slowing of fast alpha particles on each flux surface in the plasma. The fusion heating component of the BALDUR code also computes the production rate of thermal helium ions and the depletion rates of deuterium and tritium ions within the plasma core.

2.1 Mixed Bohm gyroBohm (mixed B/gB)

The mixed B/gB anomalous core transport model [14] can be expressed as follows:

$$\chi_e = 1.0\chi_{gB} + 2.0\chi_B \quad (1)$$

$$\chi_i = 0.5\chi_{gB} + 4.0\chi_B + \chi_{neo} \quad (2)$$

$$D_H = [0.3+0.7\rho]\frac{\chi_e\chi_i}{\chi_e+\chi_i} \quad (3)$$

$$D_Z = D_H \quad (4)$$

where,

$$\chi_{gB} = 5\times10^{-6}\sqrt{T_e}\left|\frac{\nabla T_e}{B_T^2}\right| \quad (5)$$

$$\chi_B = 4\times10^{-5}R\left|\frac{\nabla(n_eT_e)}{n_eB_\phi}\right|q^2\left(\frac{T_{e,0.8}-T_{e,1.0}}{T_{e,1.0}}\right) \quad (6)$$

the χ_e is the electron diffusivity (m^2/s), χ_i is the ion diffusivity (m^2/s), D_H is the particle diffusivity (m^2/s), D_z is the impurity diffusivity (m^2/s), χ_{gB} is the gyro-Bohm contribution, χ_B is the Bohm contribution, ρ is normalized minor radius, T_e is the local electron temperature (eV), B_ϕ is the toroidal magnetic field (T), R is the major radius (m), n_e is the local electron density ($x10^{20}$ m^{-3}), q is the safety factor.

2.2 The suppression model[8]

The suppression model is to develop and describe a self-formation of the pedestal and the details structure of the pedestal. This model can be written as follows:

$$f_{s_x} = \frac{1}{1+C_x\left(\frac{\omega_{E\times B}}{\gamma_{ITG}}\right)^2}\times\frac{1}{\max(1,(s-0.5)^2)} \quad (7)$$

where, C_x is the optimization coefficient for each transport channel (C_i =4.32x10^3, C_e =3.91x10^3, C_H =1.19x10^2, and C_z =1.22x10^2; subscripts i , e , H , and Z stand for ion, electron, hydrogenic, and impurity, respectively), γ_{ITG} is an approximation of linear ion temperature gradient (ITG) growth rate, estimated as v_{ti}/R, in which v_{ti} is the ion thermal velocity, s is the magnetic shear, $\omega_{E\times B}$ is the flow shearing rate that is calculated by using this equation at below:

$$\omega_{ExB} = \left|\frac{RB_\theta^2}{B_\varphi}\frac{\partial\left(E_r/RB_\theta\right)}{\partial\psi}\right| \quad (8)$$

where, ψ is the poloidal flux ,and E_r can be calculated as follows:

$$E_r = \frac{1}{Zen_i}\frac{\partial p_i}{\partial r} - v_\theta B_\phi + v_\phi B_\theta \quad (9)$$

Where, $\partial p_i/\partial r$ is the pressure gradient, v_θ and v_ϕ are the poloidal and toroidal velocities, respectively, n_i is the ion density, Z is the ion charge number and e is the elementary charge. The calculation of toroidal velocity is given in

section 2.3. Note that the poloidal velocity is estimate using NCLASS module [15].

To predict a self-formation of the pedestal uses the suppression function for each transport channel as shows in Eq. (7) suppressed the anomalous core transport in every channel, which is calculated from mixed B/gB model. Thus, the suppression of ion thermal diffusivity (χ_{i_s}), the suppression of electron thermal diffusivity (χ_{e_s}), the suppression of particle diffusivity (D_{H_s}), and the suppression of impurity particle diffusivity (D_{Z_s}), are given by

$$\chi_{i_s} = \chi_i \times f_{s_{ion}} \quad (10)$$

$$\chi_{e_s} = \chi_e \times f_{s_{electron}} \quad (11)$$

$$D_{H_s} = D_H \times f_{s_{Hydrogenic}} \quad (12)$$

$$D_{Z_s} = D_Z \times f_{s_{impurity}} \quad (13)$$

2.3 Toroidal velocity model[10]

This model is assumed that toroidal velocity (v_ϕ) is directly proportional to local ion temperature (T_i), which appears as follows:

$$v_\phi = cT_i \quad (14)$$

c (=1.43x10^4) is the coefficient in the expression for toroidal velocity is determined by calibrating the model for v_ϕ against experiment data points for optimized shear *H*-mode plasma.

3. Results and Discussions

In this work, the simulations are carried out for 10 DIII-D *H*-mode discharges using the BALDUR integrated predictive modeling code. These discharges are taken from the International Profile Database [16]. Table 1 summarizes the parameters for each discharge.

The simulations results show that the predicted plasma profiles are higher than the experimental profiles due to the overpredition of the top of pedestal. The example profiles of electron temperature, ion temperature, electron density, and ion density of DIII-D discharge number 82205 are shown in Fig.1.

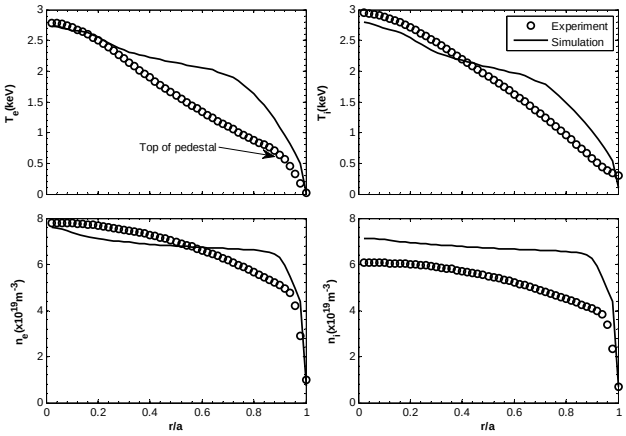

Fig.1 The profiles of electron temperature, ion temperature, electron density, and ion density as a function of normalized minor radius. The simulation results are carried out by BALDUR code, which are compared to the DIII-D discharge 82205 at the diagnostic time

Thus, to quantify and to indicate the comparison between the simulation results and experimental results, the root mean square (RMS) and offset are computed. The RMS and offset are calculated as follows:

$$\mathrm{RMS}(\%) = \sqrt{\frac{1}{N}\sum_{i=1}^{N}\left(\frac{X_{\mathrm{sim}_i} - X_{\mathrm{exp}_i}}{X_{\mathrm{exp}_0}}\right)^2} \times 100 \quad (15)$$

$$\mathrm{offset}(\%) = \frac{1}{N}\sum_{i=1}^{N}\left(\frac{X_{\mathrm{sim}_i} - X_{\mathrm{exp}_i}}{X_{\mathrm{exp}_0}}\right) \times 100 \quad (16)$$

Table. 1 Summary of plasma parameters for 10 DIII-D *H*-mode discharges at the diagnostic time.

Parameters	Discharges									
	77557	77559	81321	81329	81499	81507	82205	82788	82188	82183
R (m)	1.68	1.69	1.69	1.70	1.69	1.61	1.69	1.68	1.69	1.69
a (m)	0.62	0.62	0.60	0.59	0.63	0.54	0.63	0.62	0.63	0.54
κ	1.85	1.84	1.83	1.83	1.68	1.95	1.71	1.67	1.65	1.91
δ	0.33	0.35	0.29	0.36	0.32	0.29	0.37	0.35	0.29	0.22
B_ϕ (T)	1.99	1.99	1.98	1.94	1.91	1.91	1.87	0.94	1.57	1.57
I_p (MA)	1.00	1.00	1.00	1.00	1.35	1.34	1.34	0.66	1.33	1.33
$\bar{n}_e(10^{19}\mathrm{m}^{-3})$	4.88	5.02	2.94	5.35	4.81	4.90	5.34	2.86	6.47	6.87
Z_{eff}	1.68	2.21	2.42	1.65	2.33	1.93	2.13	1.94	1.95	1.95
P_{NB} (MW)	4.78	13.23	3.49	8.34	5.74	5.71	5.68	3.25	3.92	3.92
Time(s)	2.70	2.70	3.90	3.80	4.00	3.80	3.66	3.54	3.78	3.78

where, $X_{\exp_i}$ is the i^{th} data point of the experiment profile, X_{sim_i} is the corresponding data point of the simulation profile, and $X_{\exp_0}$ is the maximum data point of the experiment profile of X as a function of radius, which has N total number of data points. It should be note that when the offset is positive, it indicates that the simulated profile is systematically higher than the experimental profile and negative if the simulated profile is systematically lower than the experimental profile. Thus, in Figs. 2 and 3, the RMS of the electron temperature ranges from 30.78% to 13.52% in which the average value is 20.49%. In the case of ion temperature, the RMS ranges from 20.11% to 9.27% and the average RMS is 15.80%. In the case of electron density, the RMS ranges from 15.29% to 7.11% and the average value of RMS is 10.74%; moreover, the RMS value of ion density ranges from 28.11% to 10.71% and the average RMS is 17.53%. Also, the offset of four parameters are mostly positive, indicating that simulation overpredicts the experimental data.

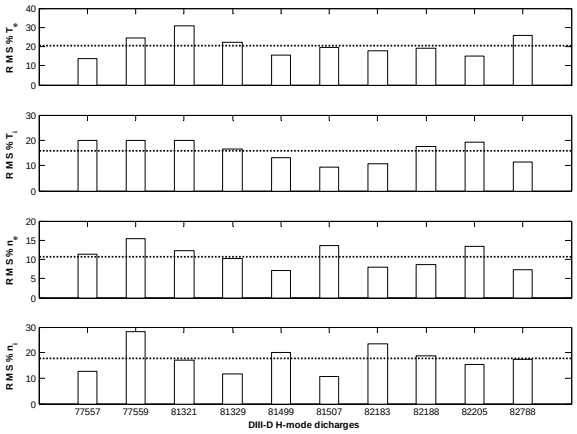

Fig.2 The RMS% for electron temperature, ion temperature, electron density, and ion density produced by simulation of BALDUR code, compared with experimental data for 10 *H*-mode discharges by DIII-D device and the average of RMS% in each profile is shown by dash line in each graph.

For this study, the RMS values and the offset values in every parameter are higher and mostly positive, when compared to the previous work in Ref.[8]. Because, the E_r as shown in Eq. (9) is

calculated from three terms, so the $\omega_{E\times B}$ flow shear is stronger than the previous work as shows in Fig. 4. Thus, all coefficients in this work must be calibrated again.

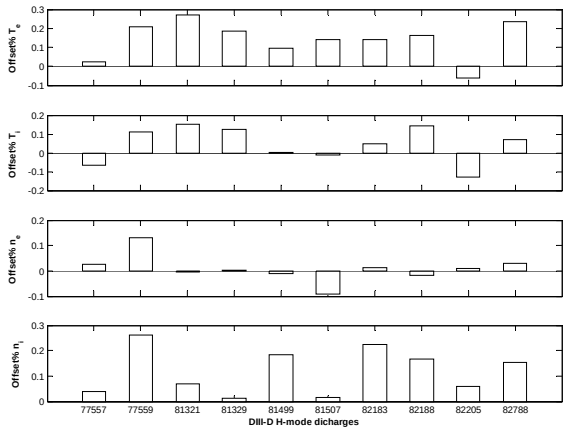

Fig.3 The offset% for electron temperature, ion temperature, electron density, and ion density produced by simulation of BALDUR code, compared with experimental data for 10 *H*-mode discharges by DIII-D device.

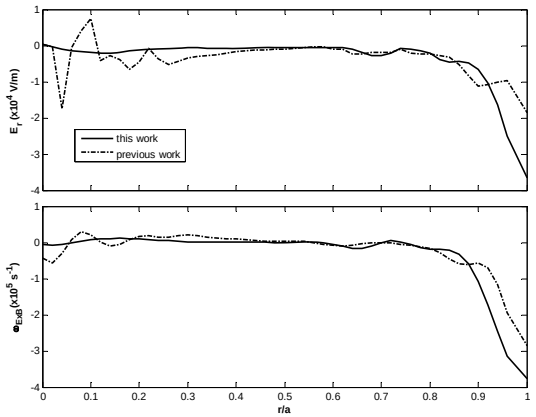

Fig.4 The simulation profiles of radial electric field (top) and $\omega_{E\times B}$ flow shear (bottom) as a function of a normalized minor radius. These simulation profiles compared two parameters between the calculation from this work and the previous work, so they are taken from DIII-D *H*-mode experiments discharge 82205.

4. Conclusion

The simulation results, which carried out by a full calculation of the radial electric field and the suppression model with all coefficients in each channel show overpredict of top pedestal. Thus, in the edge and core plasma region, the simulation results were higher than the experimental results of 10 DIII-D *H*-mode discharges as depict by RMS% and offset% values. Because, all coefficients used in this work came from the previous work, which calibrated the radial electric field of two terms; pressure gradient and poloidal velocity. To find the best prediction, all coefficients must be calibrated.

5. Acknowledgment

Authors thank Prince of Songkla University Surat Thani Campus for financial support.

6. References

[1] Connor, J. W. and Wilson, H. R. (2000). A review of theories of the L-H transition, *Plasma Physics and Controlled Fusion,* vol. 42(1), pp. R1-R74.

[2] Aymar, R., Barabaschi, P., and Shimonura, Y. (2002). The ITER design, *Plasma Physics and Controlled Fusion,* vol. 44(5), pp. 519.

[3] Hubbard, A. E. (2000). Physics and scaling of the *H*-mode pedestal, *Plasma Physics and Controlled Fusion,* vol. 42(5A), pp. A15.

[4] Biglari, H., Diamond, P. H., and Terry, P. W. (1990). Influence of sheared poloidal rotation on edge turbulence, *Physics of Fluids B: Plasma Physics,* vol. 2(1), pp. 1-4.

[5] Gohil, P. (2006). Edge transport barriers in magnetic fusion plasmas, *Comptes Rendus Physique,* vol. 7(6), pp. 606-621.

[6] Boedo, J., Gray, D., Jachmich, S., Conn, R., and Terry, G. P. (2000). Enhanced particle confinement and turbulence reduction due to ExB shear in the TEXOTR tokamak, *Nuclear Fusion,* vol. 40(7), pp. 1397.

[7] Oost, G. V., Adámek, J., Antoni, V., Balan, P., Boedo, J. A., Devynck, P.*, et al.* (2003). Turbulent transport reduction by E × B velocity shear during edge plasma biasing: recent experimental results, *Plasma Physics and Controlled Fusion,* vol. 45(5), pp. 621.

[8] Pianroj, Y., Techakunchaiyanunt, J., and Onjun, T. (2012). Model for Pedestal Transport Based on Suppression of Anomalous Transport Uning w_{ExB} Flow Shear and Magnetic Shear, *Journal of the Physical Society of Japan,* vol. 81(044502), pp. 1-13.

[9] Pianroj, Y. and Onjun, T. (2012). Simulations of H-mode Plasma in Tokamak Using a Complete Core-Edge Modeling in the BALDUR Code, *Plasma Science and Technology,* vol. 14(9), pp. 778-788.

[10] Chatthong, B. and et al. (2010). Model for toroidal velocity in H-mode plasmas in the presence of internal transport barriers, *Nuclear Fusion,* vol. 50(6), pp. 064009.

[11] Singer, C. E., Post, D. E., Mikkelsen, D. R., Redi, M. H., McKenney, A., Silverman, A.*, et al.* (1988). Baldur: A one-dimensional plasma transport code, *Computer Physics Communications,* vol. 49(2), pp. 275-398.

[12] Onjun, T., Bateman, G., and Kritz, A. H. (2001). Comparision of low confinement mode transport simulation using mixed Bohm/gyro-Bohm and the Multi-Mode 95 transport model, *Physics of Plasmas,* vol. 8(3), pp. 975.

[13] Hannum, D., Bateman, G., Kinsey, J., Kritz, A. H., Onjun, T., and Pankin, A. (2001). Comparison of high-mode predictive simulations using Mixed Bohm/gyro-Bohm and Multi-Mode (MMM95) transport models, *Physics of Plasmas,* vol. 8(3), pp. 964-974.

[14] Tala, T., Parail, V. V., and Becoulet, A. (2002). Comparison of theory-based and semi-empirical transport modeling in JET plasmas with ITBs *Plasma Physics and Controlled Fusion,* vol. 44(5A), pp. A495.

[15] Houlberg, W. A., Shaing, K. C., Hirshman, S. P., and Zarnstorff, M. C. (1997). Bootstrap current and neoclassical transport in tokamaks of arbitrary collisionality and aspect ratio, *Physics of Plasmas,* vol. 4(9), pp. 3230.

[16] Boucher, D., Connor, J. W., Houllberg, W. A., Turner, M. F., Bracco, G., and et al. (2000). The International Multi-Tokamak Profile Database, *Nuclear Fusion,* vol. 40(12), pp. 1955.